Nuclear shadowing effects on prompt photons at ultrarelativistic energies

N. Hammon, A. Dumitru, H. Stöcker, and W. Greiner

Institut für Theoretische Physik, Robert-Mayer-Strasse 10, Johann Wolfgang Goethe-Universität,

60054 Frankfurt am Main, Germany

The transverse momentum distribution of prompt photons coming from the very early phase of ultrarelativistic heavy-ion collisions for the ultrarelativistic energies is calculated by means of perturbative QCD. We calculate the single photon cross section ($A+B\rightarrow\gamma+X$) by taking into account the partonic subprocesses $q+\bar{q}\rightarrow\gamma+g$ and $q+g\rightarrow\gamma+q$ as well as the bremsstrahlung corrections to those processes. We choose a lower momentum cutoff $k_0 = 2$ GeV separating the soft physics from perturbative QCD. We compare the results for those primary collisions with the photons produced in reactions of the thermalized secondary particles, which are calculated within scaling hydrodynamics. The QCD processes are taken in leading order. Nuclear shadowing corrections, which alter the involved nuclear structure functions are explicitly taken into account and compared to unshadowed results. Employing the GRV parton distribution parametrizations we find that at ultrarelativistic energies prompt QCD photons dominate over the thermal radiation down to transverse momenta $k_T \approx 2$ GeV. At LHC, however, thermal radiation from the quark-gluon plasma dominates for photon transverse momenta $k_T \lesssim 5$ GeV, if nuclear shadowing effects on prompt photon production are taken into account. [S0556-2813(98)05406-5]

PACS number(s): 24.85.+p, 25.75.−q, 12.38.Mh

I. INTRODUCTION

In recent years a lot of effort has been made, on the experimental as well as on the theoretical side, to investigate the physics of the quark-gluon plasma (QGP) [1]. By doing so, one hopes to gain insight into the state of hot and dense matter created in a heavy-ion collision and, in a more general manner, to learn about the evolution of the early universe which is believed to have passed this state shortly after the big bang. During the time when the matter, produced in the collision of two heavy nuclei at very high energies, is in the quark-gluon phase, particles stemming from the interaction between the plasma constituents will arise. By detecting the produced particles one hopes to gain knowledge of the physics of the QGP. Those signatures for the plasma can be dilepton production, J/ψ suppression, and photon production (for a review, see [2]). It is important to know the contribution from collisions between the initial nucleons, i.e., from a non-plasma source, giving a background contribution to the thermal yield.

In this publication we consider prompt photon production via the QCD processes $q+\bar{q}\rightarrow\gamma+g$ and $q+g\rightarrow\gamma+q$ and by their bremsstrahlung contributions up to $\mathcal{O}(\alpha_s^2)$ at midrapidity to investigate by which amount nuclear effects as shadowing contribute to the hard process. We take the formulas in leading-order and simulate the higher-order terms by a K factor. In order to get information about the primary γ's one needs reliable information about the infrared-dominated quantities entering the cross sections, i.e., the parton distribution functions. The uncertainties appearing in connection with the QCD cross sections in nuclei are two-fold. Not only one has to deal with the low-x behavior of the parton distribution functions but also it is unavoidable to account for modifications of those distributions in nuclei, such as shadowing corrections, especially when considering

heavy nuclei such as Pb and Au. We consider photon transverse momenta in the range $k_T = 2-5$ GeV which is relevant for the QGP (it was suggested [3] that in the region $k_T = 2-4$ GeV the thermal photons from the QGP may dominate whereas the hard QCD γ's should dominate the larger k_T region). The hard collisions take place at some time $\tau \approx 1/k_0 \approx 0.1$ fm/c. The typical time scale for the QGP formation requires knowledge of the dynamics of the formation and equilibration of the plasma. We therefore employ two sets of initial conditions for the temperature and the proper time in the hydrocalculations to obtain a lower and an upper bound for the thermal yield.

II. INCLUSIVE SINGLE PHOTON PRODUCTION IN QCD

We first consider the cross section of single γ production on the nucleon-nucleon level. The general form of a factorized inclusive cross section with large momentum transfer k_T can be written as [4]

$$\sigma(k_T) = H_0 \otimes f_2 \otimes f_2 + (1/k_T)H_1 \otimes f_2 \otimes f_3 + (1/k_T^2)H_2 \otimes f_2 \otimes f_4 + \mathcal{O}(1/k_T^3), \tag{1}$$

where the process at the nucleon nucleon level is

$$N(P,S) + N'(P',S) \rightarrow \gamma(k) + X \tag{2}$$

as illustrated in Fig. 1. The convolution is formulated in terms of the momentum fractions x and y. The f_n are infrared-dominated nonperturbative matrix elements of twist n and the H_i are the perturbatively calculable coefficient functions. In our approach we will work in LO with a K factor for the higher orders in α_s and at the twist-2 level. The next twist to contribute in an unpolarized process would be twist-4 which is suppressed by $\mathcal{O}(1/k_T^2)$ compared to the
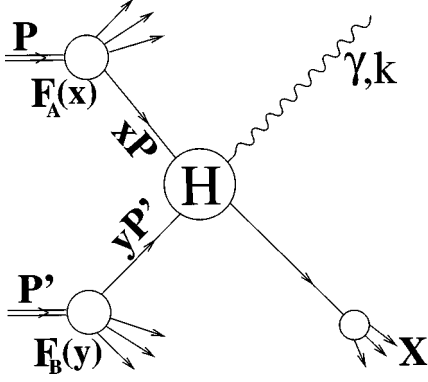
FIG. 1. General illustration of the direct single photon reaction. The square of F_A and F_B generates the nucleon matrix element and H is the hard part of the reaction involving the different partonic subprocesses.

leading twist and is therefore neglected. Matrix elements of twist-3 contribute only to polarized processes, such as single-spin asymmetries [4,5].

On the twist-2 level the cross section is

$$E_c \frac{d\sigma}{d^3 k_c}(AB \rightarrow CX) = \frac{1}{\pi} \sum_{ab \rightarrow cd} \int dx_a \ dx_b \ f^a_A(x_a) f^b_B(x_b)$$

$$\times \hat{s} \ \frac{d\hat{\sigma}}{d\hat{t}}(ab \rightarrow cd) \ \delta(\hat{s}+\hat{t}+\hat{u}), \quad (3)$$

where the sum runs over all partonic subprocess including quark-antiquark annihilation into two photons and into photon and gluon and the QCD Compton process. As stated above, we are here only interested in the *single* photon processes. Reactions involving two final-state photons, such as $q + \bar{q} \rightarrow \gamma + \gamma$, are neglected since they are suppressed due to the additional electromagnetic coupling constant. Some comments on Bremsstrahlung will appear later because one gets a large contribution from those processes.

Since the above formula applys for the twist-2 level, the $f_{A,B}$ are the well-known parton distribution functions of definite twist. For our calculations we used the newest version of the Glück, Reya, and Vogt parametrizations [6]. The main reason for choosing the newest version is the modifications at small x measured at HERA [7] which show a steep rise in the proton structure function $F_2(x,Q^2)$. The photons at midrapidity typically come from momentum fractions $x \approx 2k_0/\sqrt{s}$. Therefore, at the high-energy colliders treated here (RHIC and LHC) one clearly is in a region where new data on parton distributions at low x are important. Another interesting property of the '95 GRV parametrizations is the asymmetric sea taking into account the violation of the Gottfried sum rule, which defines the difference between the proton and neutron structure functions [8]:

$$I_{GSR} = \int_0^1 \frac{dx}{x}(F^p_2 - F^n_2) = \frac{1}{3}\int_0^1 dx(u_v - d_v) + \frac{2}{3}\int_0^1 dx(\bar{u} - \bar{d})$$

$$= \frac{1}{3} \quad \text{if} \quad \bar{u} = \bar{d}. \quad (4)$$

The early analysis (prior to 1992) assumed a flavor-independent light-quark sea. The NMC collaboration, on the contrary, found [9]

$$\Sigma(0.004,0.8) = \int_{0.004}^{0.8} \frac{dx}{x}(F^p_2 - F^n_2)$$

$$= 0.227 \pm 0.007 \ (\text{stat.}) \pm 0.014 \ (\text{syst.}) \quad (5)$$

implying $\bar{d} \geq \bar{u}$.

The (unpolarized) cross section for the prompt photon production in a nucleus nucleus reaction is given (without the exchange term) to lowest order by [10]

$$E_k \frac{d\sigma^{AB}}{d^3 k}[A+B \rightarrow \gamma(k)+X]$$

$$= \frac{1}{\pi}\int_{x^a_{min}}^1 dx_a f^A_i(x_a) f^B_j(x_b) \frac{x_a x_b}{x_a - x_1}\frac{d\hat{\sigma}}{d\hat{t}}(a+b \rightarrow c+d),$$

$$(6)$$

where $f^A_i(x_a)$ and $f^B_j(x_b)$ are the parton distributions *in the nucleus*. The various hard scattering functions can, e.g., be found in [11]

$$\frac{d\hat{\sigma}}{d\hat{t}} = \frac{\pi\alpha\alpha_s e^2_q}{\hat{s}^2}\frac{2}{3}\left[\left(\frac{\hat{s}}{-\hat{t}}\right)+\left(\frac{-\hat{t}}{\hat{s}}\right)\right], \quad (7)$$

$$\frac{d\hat{\sigma}}{d\hat{t}} = \frac{\pi\alpha\alpha_s e^2_q}{\hat{s}^2}\frac{8}{9}\left[\left(\frac{\hat{u}}{\hat{t}}\right)+\left(\frac{\hat{t}}{\hat{u}}\right)\right] \quad (8)$$

for the processes $q + g \rightarrow \gamma + q$ and $q + \bar{q} \rightarrow \gamma + g$, respectively.

The partonic variables at midrapidity are given by

$$x_b = \frac{x_a x_T}{2x_a - x_t}, \quad x_T = 2k_T/\sqrt{s},$$

$$x_a = x_b = k_T/\sqrt{s}, \quad x^{min}_a = \frac{x_T}{2 - x_T}, \quad (9)$$

$$\hat{s} = x_a x_b s, \quad \hat{u} = -x_b x_T s/2, \quad \hat{t} = -x_a x_T s/2. \quad (10)$$

We also explicitly take the $\mathcal{O}(\alpha^2_s)$ corrections to the annihilation and Compton graphs, i.e., bremsstrahlung contribu-

tions, into account. Even though one has a $\mathcal{O}(\alpha_s^2)$ contribution, these processes already contribute to $\mathcal{O}(\alpha_s)$ because the fragmentation function enters with a factor $\ln(Q^2/\Lambda^2)$.

In that process a photon is radiated off a final state quark, or in other words: the quark fragments into a photon carrying a fraction z of the initial momentum. The fragmentation function is given in leading-log approximation by [11]

$$zD_{q\to\gamma}(z,Q^2)=e_q^2\frac{\alpha}{2\pi}[1+(1-z)^2]\ \ln(Q^2/\Lambda^2).\quad(11)$$

The result for the bremsstrahlung contributions is given by [11]

$$E_k\frac{d\sigma^{AB}}{d^3k}=2\frac{\alpha\alpha_s^2}{2\pi s^2}\ln\frac{k_T^2}{\Lambda^2}\frac{1}{x_T}\int_{x_T}^1 dy_T\frac{4}{y_T^2}[1+(1-x_T/y_T)^2]\int_{y_T/(2-y_T)}^1\frac{dx_a}{x_a-y_T/2}\Bigg[F_2(x_a,A)\bigg(xG(x_b,B)$$

$$+\frac{4}{9}Q(x_b,B)\bigg)\frac{x_a^2+(y_T/2)^2}{x_a^4}+(x_a\leftrightarrow x_b,A\leftrightarrow B)\Bigg],\quad(12)$$

where $x_b=x_ay_T/(2x_a-y_T)$ and $Q(x)=x\Sigma_f[q_f(x)+\bar{q}_f(x)]$. The graphs giving rise to the different hard parts are shown in Fig. 2. Notice that an expression $[xG(x_b,B)+(4/9)Q(x_b,B)]$ appears. This so-called *effective parton*
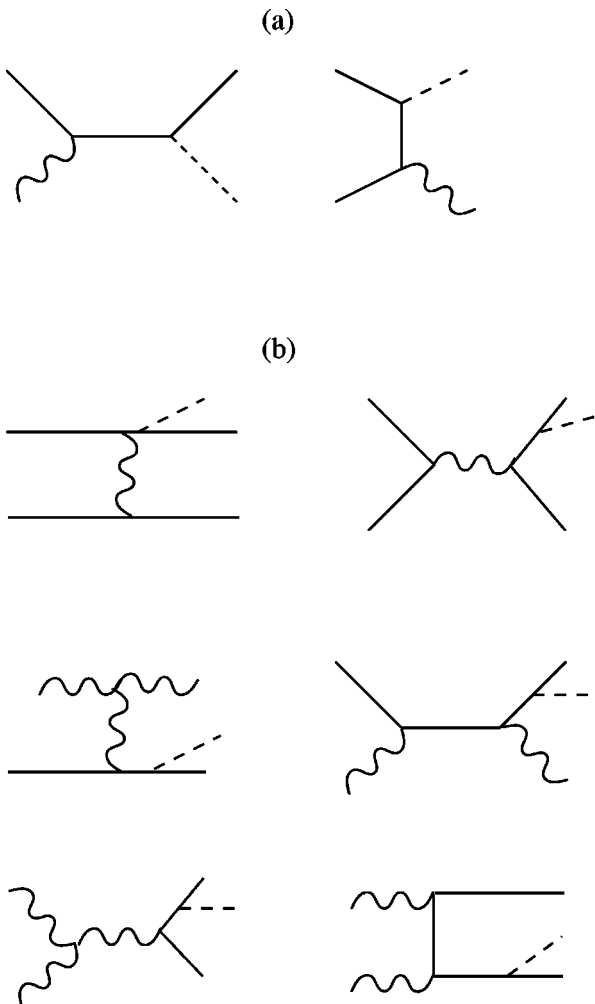
(a)

(b)

FIG. 2. (a) QCD Compton, annihilation and (b) Bremsstrahlung graphs taken into account in our calculations. The wavy lines denote gluons and the dashed lines stand for the photons.
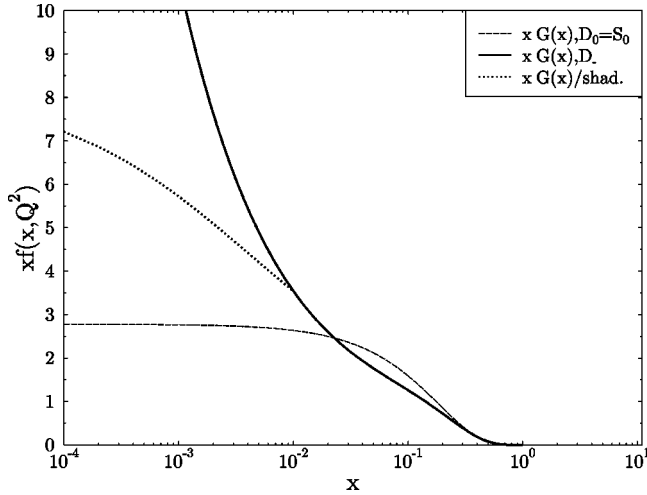
distribution is due to the different values of the following subprocesses:

$$qq\to qq\ :\ qg\to qg\ :\ gg\to gg$$

$$\approx 1\ :\ C_A/C_F\ :\ (C_A/C_F)^2.\quad(13)$$

One therefore is able to describe the whole process in terms of a *single effective subprocess* with an *effective* parton distribution

$$Q'(x)=xG(x)+\frac{C_F}{C_A}Q(x)$$

$$=xG(x)+\frac{C_F}{C_A}x\sum_f\ [q_f(x)+\bar{q}_f(x)]\quad(14)$$

with $C_F/C_A=4/9$.

In the next section we will discuss modifications to the cross section due to nuclear effects.

III. MODIFICATIONS OF THE CROSS SECTION: NUCLEAR SHADOWING

For the case of prompt photon production in a nucleus-nucleus reaction one has to deal with *nuclear* parton distributions entering the cross section, $xG^A(x,Q^2)$ and $F_2^A(x,Q^2)$. It is well known from eA, μA, and pA scattering [12–14] that over the whole x range, one finds $f_i^A(x,Q^2)\neq Af_i^P(x,Q^2)$ for the parton densities. Here one has nuclear shadowing, antishadowing, the EMC effect and Fermi motion, depending on the increasing x region [15]. In the present case we are mainly interested in the small-x region, i.e., in shadowing. At midrapidity one typically probes the correlators down to momentum fractions $x\approx k_T\sqrt{s}/(1-k_T\sqrt{s})$. Thus in the interesting k_T range at RHIC one reaches values $x\approx 0.01$ and $x\approx 3.4\times 10^{-4}$ at LHC.

The shadowing effect described here is a depletion of the parton densities in the nucleus. This effect can be understood in terms of parton-parton fusion in the infinite-momentum frame [16]. If the longitudinal wavelength of a parton exceeds the contracted size of a nucleon (or the internucleon

FIG. 3. Depletion of $xG(x)$ in the proton as parametrized by MRS in [17]. The D_- curve corrsponds to a singular behavior ($\sim x^{-0.5}$) as postulated by BFKL analysis whereas the small x behaviors of S_0 is taken from Regge anyalysis ($\sim x^0$).

distance) inside the Lorentz contracted nucleus, partons originating from different nucleons can fuse, resulting in a depletion of the parton densities at smaller x and in an enhancement at larger x. One finds from $1/xP \approx 2R_n M_n / P$ that shadowing shows up at values $x \approx 0.1$. A saturation of the shadowing effect can be expected when the longitudinal parton wavelength exceeds the size of the nucleus.

One also expects a shadowing effect from a transverse overlap of the partons as is seen in the free proton. Here one finds that, for sufficiently small values of x and/or Q^2, the total transverse area occupied by gluons becomes larger than the transverse area of the hadron. This happens when $xG(x) \gtrsim Q^2 R^2$, with a transverse parton size $1/Q^2$ ($Q^2 = -q^2$) and a proton radius R. Hence, one finds a depletion of the gluon and sea distribution at values $x \lesssim 0.01$ as shown in Fig. 3.

It is obvious that shadowing depends, on the one hand, on the mass number of the nucleus and, on the other hand, on the x and Q^2 values. The Q^2 dependence of the ratio $(1/A)f_i^A(x,Q^2)/f_i^P(x,Q^2)$ is determined by modified DGLAP equations (suggested in [18] and later proven in [16]) taking the fusion processes into account [19]. In the nucleus those fusion processes are due to an enhancement of the fusion of gluon ladders stemming from independent partons, whereas in the free nucleon, fusion processes from non-independent partons dominate.

It was shown [20] that the modifications to the usual DGLAP equations only affect the ratio by $\approx (6-7)\%$. Because the detected photons are in a quite narrow range of k_T where $k_T^2 \approx Q^2$, for simplicity, a parametrization for both $G^A(x,Q^2)$ and $F_2^A(x,Q^2)$ is used. The first ansatz [20] assumes a similar size of the shadowing of $F_2^A(x,Q^2)$ and of the gluon distribution at the initial scale $Q_0 = 2$ GeV. The evolution of $F_2(x,Q^2)$ is quite moderate, whereas the gluon shadowing vanishes faster with increasing Q^2. This can be understood in terms of the momentum flow into gluons at higher Q^2 as predicted by the DGLAP equations.

The parametrization of the $(1/A)F_2^A(x,Q^2)/F_2^P(x,Q^2)$ ratio at the input scale, $Q_0 = 2$ GeV, given in [20], is shown in
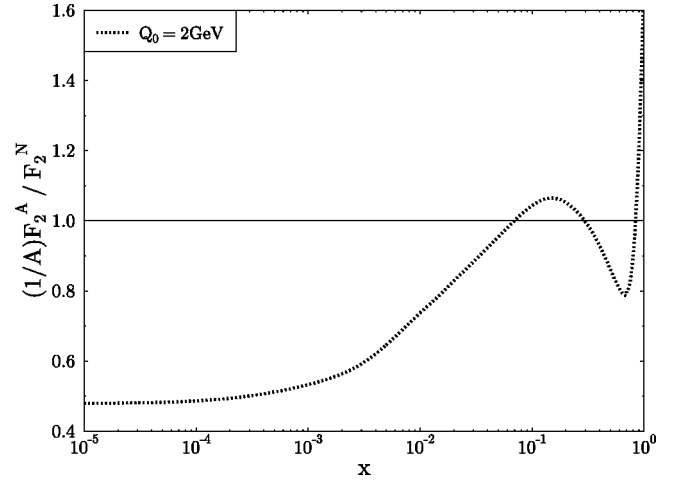

FIG. 4. Ratio $(1/A)F_2^A(x,Q^2)/F_2^P(x,Q^2)$ at the input scale $Q_0 = 2$ GeV as parametrized in [20].

Fig. 4. Nevertheless, the same parametrization for both distributions is used, so one does not need to solve the modified DGLAP equations for the narrow k_T range. It is clear that thereby the shadowing effect is slightly overestimated when one tries to be consistent in one ansatz.

Due to the electromagnetical neutrality, the $R_G(x,Q^2)$ ratio is not accessible with deep inelastic-scattering processes. A second ansatz [20] with a much stronger shadowed gluon distribution [$R_G(x,Q^2)$ is roughly 45% smaller than R_{F_2} at $x = 0.001$] has been presented at the initial value $Q = Q_0 = 2$ GeV. The neglect of the Q^2 dependence of $R_G(x,Q^2)$ is absorbed by the systematic uncertainty in the ansatz. But there definitely remains an overestimate due to the neglect of the Q^2 dependence of $R_{F_2}(x,Q^2)$ which changes by $\approx 9\%$ as Q varies from 2 to 5 GeV at $x = 0.001$. Therefore, our overestimate alters the result towards larger k_T by $\approx 10\%$.

We show the effect of shadowing for the two energies $\sqrt{s} = 200A$ GeV and $\sqrt{s} = 5.5A$ TeV in Figs. 5 and 6. The shadowing effect increases as the energy increases which can easily be understood in terms of the momentum fraction: as one typically probes the correlators (here the parton distribution functions entering the hand-bag graph) at values x
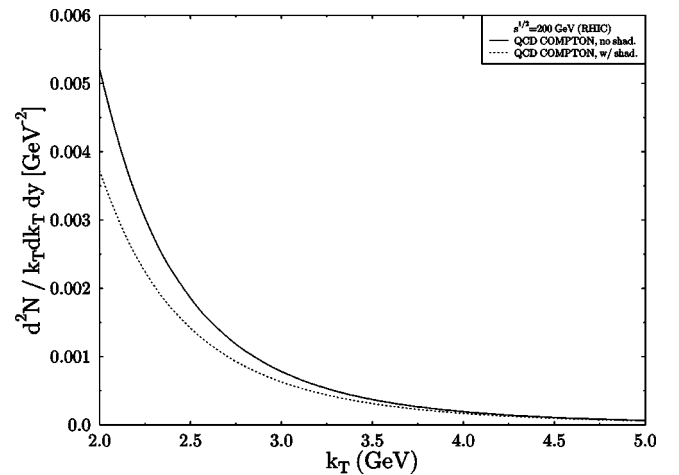

FIG. 5. QCD Compton photon multiplicity distribution with and without nuclear shadowing for $\sqrt{s} = 200A$ GeV.
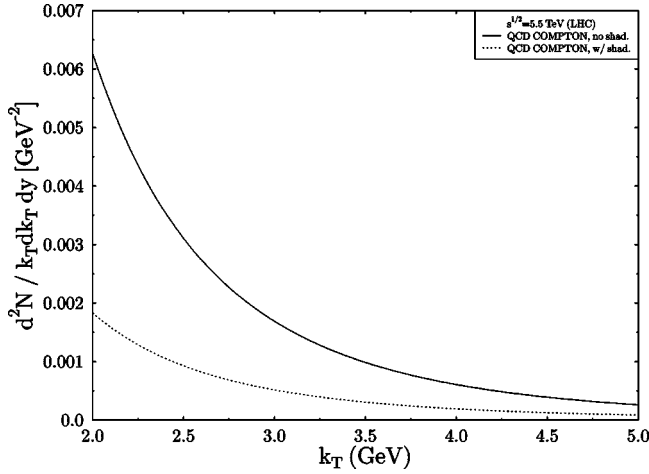
FIG. 6. Same as Fig. 5 but for $\sqrt{s} = 5.5A$ TeV.

$\approx 2k_T/\sqrt{s}$ at $y = 0$, this formula also immediately explains the drop of the ratio towards larger transverse momenta. The decrease of the shadowing correction with increasing k_T can also be understood in terms of the lower integration boundary x^a_{min} in Eq. (6) which increases with the transverse momentum of the photon.

Each cross section is computed on the nucleon-nucleon level as $d\sigma_{pp}/dy$. Then this quantity is transformed to the number of events per rapidity in a central nucleus-nucleus reaction by multiplying with the nuclear overlap function $T_{AA}(b)$ at zero impact parameter:

$$\frac{dN_{AA}}{dy} = T_{AA}(\mathbf{b}=0)\frac{d\sigma_{pp}}{dy}. \qquad (15)$$

One should not forget that the results for *central* collisions are about four times larger than those for collisions *averaged* over all impact parameters.

Numerically one finds that $T_{AA}(\mathbf{b}=0) \approx A^2/\pi R_A^2$,

$$T_{PbPb} = \frac{32}{mb}, \qquad T_{AuAu} = \frac{29}{mb}. \qquad (16)$$

This procedure is equivalent to neglecting nuclear shadowing effects. To explicitly take into account those effects one has to multiply each parton distribution with the parametrized ratio $R_{F_2} = (1/A)F_2^A/F_2^N$.

IV. THE HYDRODYNAMICAL CALCULATIONS

For comparison we have also computed the transverse momentum spectrum of *thermal* hard photons. As a model for the time evolution of the thermalized system we assume a three-dimensional hydrodynamical expansion with cylindrical symmetry and longitudinal boost invariance [21]. For the RHIC energy we employ an initial temperature of $T_i = 533$ MeV and an initial time of $\tau_i = 0.1236$ fm/c, while for LHC we assume $T_i = 880$ MeV and $\tau_i = 0.1$ fm/c. The resulting final pion multiplicity in central Au+Au reactions (i.e., initial transverse QGP radius $R_T = 6.5$ fm) is $dN^\pi/dy \approx 1460$ at RHIC and $dN^\pi/dy \approx 5300$ at LHC, if the hydrodynamical evolution is isentropic and if the QGP and the hadron gas consists of u, d quarks, gluons and pions, respec-

tively [22]. According to present knowledge [23,24], from the viewpoint of maximum thermal radiation these initial conditions (and the assumption of full thermal and chemical equilibrium) have to be considered as the most favorable ones. Therefore, we have also computed the thermal photon spectrum for a less rapid thermalization and a lower initial temperature ($\tau_i = 0.5$ fm/c, $T_i = 300$ MeV, $dN^\pi/dy \approx 1050$ for RHIC and $\tau_i = 0.25$ fm/c, $T_i = 650$ MeV, $dN^\pi/dy \approx 5350$ for LHC). We assume a freeze-out temperature of $T_f = 100$ MeV. The photon spectrum above $k_T = 2$ GeV, however, does not depend sensitively on this number, except in the case of slow thermalization and low initial temperature ($\tau_i = 0.5$ fm/c, $T_i = 300$ MeV).

The equation of state is that of an ideal gas of massive π, η, ρ, and ω mesons below $T_C = 160$ MeV. For $T > T_C$ we assume an ideal QGP (massless, noninteracting u, d quarks and gluons) described within the MIT bag-model. The bag constant is chosen such that the pressures of the two phases match at $T = T_C$ ($B^{1/4} = 235$ MeV) thus leading to a first-order phase transition.

The number of emitted direct photons per infinitesimal space-time volume in each of the three phases is parametrized as [25,26]

$$E\frac{dN^\gamma}{d^4x\,d^3k} = \frac{5\alpha\alpha_S}{18\pi^2}T^2 e^{-E/T}\ln\left(\frac{2.912E}{g^2T}+1\right). \qquad (17)$$

E is the photon energy in the local rest frame. In our hydrocalculations we fix $\alpha_s = g^2/4\pi = 0.3$. A logarithmic temperature dependence of α_s does not alter the results significantly. Equation (17) accounts for pion annihilation ($\pi\pi \to \rho\gamma$), and Compton-like scattering ($\pi\rho \to \pi\gamma$, $\pi\eta \to \pi\gamma$) off a ρ or η meson (in lowest-order perturbation theory). In the QGP (two massless flavors), alternatively, quark-antiquark annihilation ($q\bar{q} \to g\gamma$), and Compton-like scattering off a gluon ($q,\bar{q}+g \to q,\bar{q}+\gamma$) are considered. In view of the uncertainties of the initial conditions and the time evolution of the temperature, which enters the thermal photon production rate exponentially, we have not attempted to include higher-order corrections, hadronic form factors, or additional processes (e.g., $a_1 \to \pi\gamma$ decays, etc.). Finally, the thermal photons produced at each individual space-time point are summed incoherently to obtain the spectrum of photons emitted in a nuclear collision.

V. RESULTS

We have calculated the transverse momentum spectrum (at midrapidity) of prompt photons, $d^2N^\gamma/k_T dk_T dy$ produced in the very early phase ($1/k_0 \approx 0.1$ fm/c) of an ultrarelativistic heavy-ion collision via perturbative QCD. We take the transverse photon momenta in the range $k_T = 2-5$ GeV. The lower bound is chosen such that perturbation theory is still valid and one does not have to take into account matrix elements of higher twist, such as $\langle P|F^{+\alpha}\bar{\psi}\gamma^+ F^+_\alpha \psi|P\rangle$. We use a rather moderate estimate for the higher-order terms, namely $K = 1.5$ for RHIC and $K = 1.0$ for LHC. We compare those prompt photons to the thermal radiation, calculated as outlined above (cf. Figs. 7 and 9). In the relevant range we find that the photons from bremsstrahlung dominate over
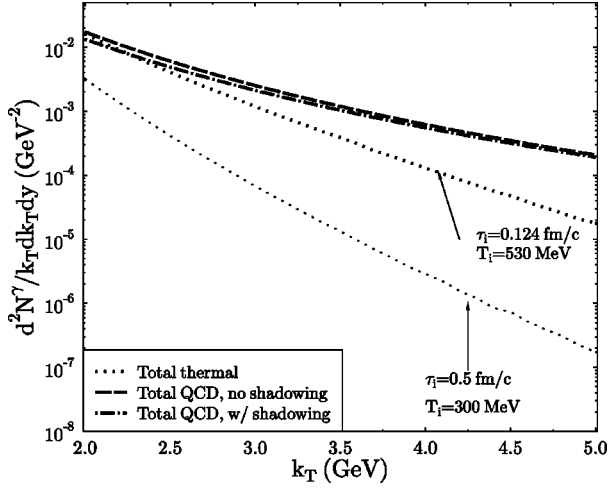
FIG. 7. Transverse momentum distribution of prompt and thermal photons produced in a central Au+Au collision at $\sqrt{s} = 200A$ GeV.

those coming from the QCD Compton process by a factor $\approx 1.6[\ln(1/x_T) - 1.1]$, which itself dominates over the annihilation process as also found in [11] and [22]. In our calculation we find that the Bremsstrahlung contribution at RHIC lies above the Compton contribution in the whole k_T range whereas in [11] one had a crossover point at $k_T \approx 3.5$ GeV. This different behavior should be due to the parton distributions (Duke/Owens set I) used in [11]. Also, for the parton distributions employed by us, prompt photons dominate over the thermal radiation in the entire transverse momentum range at RHIC, cf. Fig. 7. The inverse slope $1/T = -d/dk_T \ln (dN/k_T dk_T dy)$ of the prompt QCD photons in the interval $k_T = 2-5$ GeV is $T = 500-1000$ MeV at RHIC and $T = 500-1100$ MeV at LHC, depending on k_T. Hydrodynamics predicts that the inverse slope of the thermal photons can hardly exceed 500 MeV at RHIC and 700 MeV at LHC, even if very rapid thermalization times $\tau_i \approx 1/k_0$ and high initial temperatures $T_i \approx 3\langle E_T \rangle$ are assumed. The effect of the nuclear shadowing correction is quite moderate at the RHIC energy as also found in minijet calculations [20]. Note
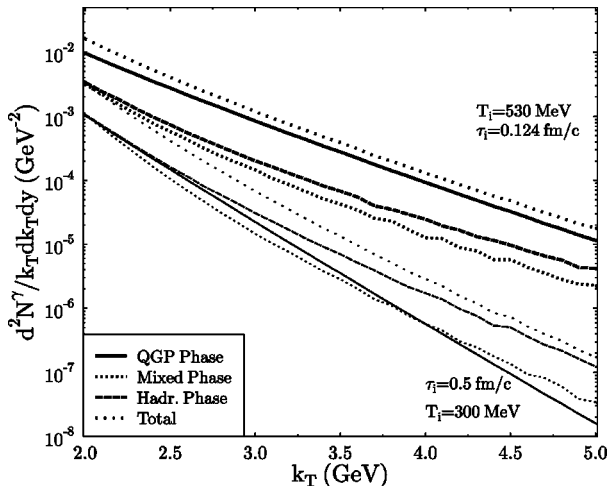

FIG. 8. Transverse momentum distribution of thermal photons produced in the different phases at $\sqrt{s} = 200A$ GeV with different initial conditions.
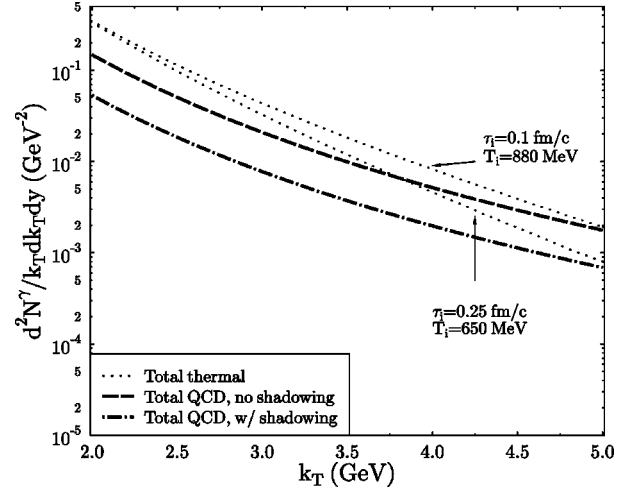

FIG. 9. Same as Fig. 7 but for $\sqrt{s} = 5.5A$ TeV in Pb+Pb.

also (Fig. 8) that for the second set of initial conditions the hadronic phase dominates the thermal photon spectrum, due to the strong radial flow. A higher freeze-out temperature would, however, reduce this contribution.

The effect of nuclear shadowing increases for higher energies (LHC, see Fig. 9) and yields corrections up to a factor of ≈ 3.5, and therefore is not negligible, especially at smaller momentum fractions. Without shadowing corrections one has a crossover point with the thermal yield ($\tau_i = 0.25$ fm, $T_i = 650$ MeV) at $k_T \approx 3.75$ GeV. When taking into account the shadowing corrections one finds the crossover point at larger transverse momenta ($k_T \approx 5$ GeV). For the higher initial temperature of $T_i = 880$ MeV, the crossover point is shifted to even larger values of k_T.

Thus, even for the lower initial temperature and larger formation time, photons from primary QCD processes in the important range $k_T = 2-5$ GeV are negligible at LHC if shadowing is taken into account. Also, for the initial conditions expected at LHC, the thermal spectrum is dominated by photons produced in the QGP phase (Fig. 10).

A comment regarding the photons from hadron decays, mostly from π^0 and η decays, is appropriate at this point. This background radiation is discussed, e.g., in [24,26] and
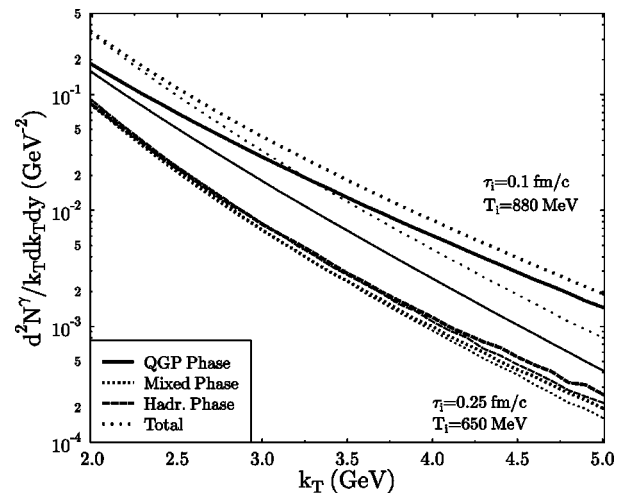

FIG. 10. Same as Fig. 8 but for $\sqrt{s} = 5.5A$ TeV.

turns out to exceed the thermal yield in the transverse momentum range considered here. Therefore, it has been argued [24] that these decay photons have to be identified in order for the thermal radiation to be observable. At lower energy ($\sqrt{s}=18$ GeV) this has been successfully performed by the WA98 Collaboration [27]. However, our present calculation suggests that the thermal photons will still not be observable at RHIC because the prompt QCD photons dominate the spectrum. At LHC energy, on the other hand, nuclear shadowing reduces the number of prompt QCD photons to below the thermal yield (for $k_T \lesssim 5$ GeV). Thus, thermal photons might be observable at this energy if identification of decay photons is possible.

VI. SUMMARY AND CONCLUSIONS

In this paper we have computed the number of prompt photons with 2 GeV $\leq k_T \leq 5$ GeV in a central AA collision at energies of $\sqrt{s}=200A$ GeV and $\sqrt{s}=5.5A$ TeV at midrapidity to study nuclear modifications of the naive extrapolations from pp results. We investigated different sources for the photons and also discussed thermal photon production within a hydrodynamical model and various sets of initial conditions. We used the nuclear overlap function to derive

the multiplicities from the cross sections and assumed central collisions ($\mathbf{b}=0$) which yield multiplicities about four times larger than those resulting from impact parameter-averaged calculations.

With an upper bound for nuclear shadowing and a relatively conservative estimate for the higher orders, expressed in the K factor, at RHIC we obtain multiplicities larger than those from the thermalized stage of the reaction. For the LHC energy of $\sqrt{s}=5.5A$ TeV we find that the crossover point between the thermal photons and the primary photons significantly changes towards larger transverse momenta when shadowing corrections are taken into account. Even if we slightly overestimate the shadowing effect, one can conclude that at LHC the background from QCD processes of the initial nucleons is of minor importance in the range $k_T=2-5$ GeV but will still dominate for the very high transverse photon momenta. The inverse slope of the QCD photons ($\approx 500-1000$ MeV) significantly exceeds that of the thermal photons (300–500 MeV) at RHIC and is slightly larger for LHC energies.

ACKNOWLEDGMENTS

[1] Proceedings of Quark Matter '96, edited by P. Braun-Munzinger, H. J. Specht, R. Stock, and H. Stöcker [Nucl. Phys. **A610**, 1 (1996)].
[2] J. W. Harris and B. Müller, Annu. Rev. Nucl. Part. Sci. **46**, 71 (1996).
[3] E. Shuryak, Phys. Lett. **78B**, 150 (1978).
[4] J. Qiu and G. Sterman, Nucl. Phys. **B378**, 52 (1992).
[5] N. Hammon, O. Teryaev, and A. Schäfer, Phys. Lett. B **390**, 409 (1997).
[6] M. Glück, E. Reya, and A. Vogt, Z. Phys. C **67**, 433 (1995).
[7] M. Derrick et al., Phys. Lett. B **316**, 515 (1993).
[8] K. Gottfried, Phys. Rev. Lett. **18**, 1174 (1967).
[9] P. Amaudruz et al., Phys. Rev. Lett. **66**, 2712 (1991).
[10] R. Field, Applications of Perturbative QCD (Addison-Wesley, Reading, MA, 1989).
[11] J. Alam, D.K. Srivastava, B. Sinha, and D.N. Basu, Phys. Rev. D **48**, 1117 (1993).
[12] R.G. Arnold et al., Phys. Rev. Lett. **52**, 727 (1984).
[13] NM Collaboration, P. Amaudruz et al., Z. Phys. C **51**, 387 (1991).
[14] D.M. Alde et al., Phys. Rev. Lett. **64**, 2479 (1990).
[15] L. Frankfurt and M. Strikman, Phys. Rep. **160**, 235 (1988).
[16] A.H. Müller and J. Qiu, Nucl. Phys. **B268**, 427 (1986).
[17] A.D. Martin, W.J. Stirling, and R.G. Roberts, Phys. Rev. D **47**, 867 (1993).
[18] L. Gribov, E. Levin, and M. Ryskin, Phys. Rep. **100**, 1 (1983).
[19] K. Eskola, J. Qiu, and X. Wang, Phys. Rev. Lett. **72**, 36 (1994).
[20] K. Eskola, Nucl. Phys. **B400**, 240 (1993).
[21] K. Kajantie and L. McLerran, Phys. Lett. **119B**, 203 (1982); Nucl. Phys. **B214**, 261 (1983); J.D. Bjorken, Phys. Rev. D **27**, 140 (1983); G. Baym, B.L. Friman, J.P. Blaizot, M. Soyeur, and W. Czyz, Nucl. Phys. **A407**, 541 (1983); K. Kajantie, R. Raitio, and P.V. Ruuskanen, Nucl. Phys. **B222**, 152 (1983); H. von Gersdorff, M. Kataja, L. McLerran, and P.V. Ruuskanen, Phys. Rev. D **34**, 794 (1986).
[22] R.C. Hwa and K. Kajantie, Phys. Rev. D **32**, 1109 (1985).
[23] X.N. Wang and M. Gyulassy, Phys. Rev. D **44**, 3501 (1991); B. Müller and X.N. Wang, Phys. Rev. Lett. **68**, 2437 (1992); K. Geiger, Phys. Rev. D **46**, 4965 (1992); J. Kapusta, L. McLerran, and D.K. Srivastava, Phys. Lett. B **283**, 145 (1992); E. Shuryak, Phys. Rev. Lett. **68**, 3270 (1992); T.S. Biro, E. van Doorn, B. Müller, M.H. Thoma, and X.N. Wang, Phys. Rev. C **48**, 1275 (1993); E. Shuryak and L. Xiong, Phys. Rev. Lett. **70**, 2241 (1993); K.J. Eskola and X.N. Wang, Phys. Rev. D **49**, 1284 (1994); B. Kämpfer and O.P. Pavlenko, Z. Phys. C **62**, 491 (1994); J.J. Neumann, D. Seibert, and G. Fai, Phys. Rev. C **51**, 1460 (1995); X.N. Wang, Nucl. Phys. **A590**, 47c (1995); K.J. Eskola and K. Kajantie, Z. Phys. C **75**, 515 (1997); K.J. Eskola, K. Kajantie, and P.V. Ruuskanen, Eur. J. Phys. **C1**, 627 (1998); D.K. Srivastava, M.G. Mustafa, and B. Müller, Phys. Rev. C **56**, 1064 (1997).
[24] D.K. Srivastava, B. Sinha, M. Gyulassy, and X.N. Wang, Phys. Lett. B **276**, 285 (1992).
[25] J. Kapusta, P. Lichard, and D. Seibert, Phys. Rev. D **44**, 2774 (1991); R. Baier, H. Nakkagawa, A. Niegawa, and K. Redlich, Z. Phys. C **53**, 433 (1992).
[26] P.V. Ruuskanen, Nucl. Phys. **A544**, 169c (1992).
[27] T. Peitzmann and the WA98 Collaboration, Proceedings of Quark Matter '97 [Nucl. Phys. A (to be published)].